Available online at BCREC Website: http://bcrec.undip.ac.id

Bulletin of Chemical Reaction Engineering & Catalysis, 11 (2), 2016, 161-169

Research Article

Phy-chemical Attributes of Nano-scale V_2O_5/TiO_2 Catalyst and Its' Effect on Soot Oxidation

Deqing Mei[1]*, Lichang Li[1], Chen Zhu[1], Xiang Zhao[1], Yinnan Yuan[2]

[1]*School of Automobile and Traffic Engineering, Jiangsu University, Zhenjiang, Jiangsu 212013, China*
[2]*School of Energy, Soochow University, Suzhou, Jiangsu 215006, China*

Received: 25th October 2015; Revised: 25th December 2015; Accepted: 5th January 2016

Abstract

The V_2O_5 catalysts which supported on nano-scale TiO_2 with variation of vanadium contents (5%, 10%, 20% and 40%) were prepared by an incipient-wetness impregnation method. The phase structures of nano-scale V_2O_5/TiO_2 catalysts with different loading rates were characterized by Scanning electron microscope (SEM), X-Ray diffraction (XRD) and Fourier transform infrared (FT-IR) spectra. The oxidation activities of catalysts over diesel soot were performed in a themogravimetric analysis (TGA) system. The kinetics of the catalytic oxidation process were analyzed based on Flynn-Wall-Ozawa method. The characterization results showed that the phase structure of V_2O_5 supported on TiO_2 depends heavily on the vanadium contents, which will put great effects on the catalytic performances for soot oxidation. At a low vanadium loading rates (V5-V20), active species exist as monomers and polymeric states. At a high loading rate (V40), the crystalline bulk V_2O_5 covers the surface of TiO_2. The formed crystal structure occupied the active sites and led a decreasing in the catalytic effect. By comparing the characteristics temperatures of soot oxidation over V_2O_5 catalysts, the catalytic activities of catalysts with different loading rates for soot oxidation can be ranked as: V5 < V10 < V40 < V20. Via pyrolysis kinetics analysis, it is revealed that the activation energy of soot oxidation is minimum when the vanadium loading rates is 20%, which is fit well with the TG experimental results. The consistency of pyrolysis kinetics and TG experimental results confirm that the best activity catalyst is V20 in discussed catalysts of this paper, which is nearest to the monolayer dispersion saturated state of V_2O_5/TiO_2 catalyst. Moreover, it convincingly demonstrate the obvious threshold effect in V_2O_5 catalysts. Copyright © 2016 BCREC GROUP. All rights reserved

Keywords: V_2O_5/TiO_2 catalyst; phy-chemical attributes; diesel; soot; catalytic combustion

How to Cite: Mei, D., Li, L., Zhu, C., Zhao, X., Yuan, Y. (2016). Phy-chemical Attributes of Nano-scale V_2O_5/TiO_2 Catalyst and Its' Effect on Soot Oxidation. *Bulletin of Chemical Reaction Engineering & Catalysis*, 11 (2): 161-169 (doi:10.9767/bcrec.11.2.542.161-169)

Permalink/DOI: http://dx.doi.org/10.9767/bcrec.11.2.542.161-169

1. Introduction

Although diesel engines have many advantages, such as relative higher efficiency of fuel and longer durability when compared with gasoline engines, the high level of particulate matter emissions has become a problem when we satisfy the more and more strict emission regulations [1, 2]. What is more, the particulate emissions caused by incomplete combustion of fossil fuels are hazardous to the environment and human health, because of their adverse health effects on respiratory system. Currently, the combination of diesel particulate filter

---

* Corresponding Author.
E-mail: meideqing@ujs.edu.cn (D. Mei),
Telp: +86-13862445897

(DPF) with oxidation catalyst is one of the most efficient measures for reducing particulate matter emissions from diesel engines. Oxidation catalysts can significantly reduce the temperature of soot ignition and increase the rate of soot oxidation, thus realizing passive regeneration of DPF [2].

A large number of catalysts have been explored for DPF regeneration. Platinum and palladium are generally used catalysts for diesel soot combustion due to their good oxidation activity. However, the disadvantages of platinum and palladium are their high cost and production of sulfate particulates [3]. Vanadium-based catalysts have been widely employed in the field of catalysts, including the oxidative dehydrogenation of propane, selective oxidation of alcohols, oxidative degradation of volatile organic compounds (VOCs) and selective catalytic reduction (SCR) of nitrogen oxides [4-7]. In recent years, vanadium-based catalysts have been considered as the most potential one for regeneration of DPF [1, 8-10]. This is mainly attributed to its unique properties. The melting point of vanadium-based catalyst is relatively low, which may lead to forming liquid eutectic phases in the temperature range of the soot combustion reaction. The active component V_2O_5 on the carrier surface has high mobility, which can improve the loose contact state of particulate-catalyst mixtures in DPF and promote the catalytic efficiency [1, 8, 9]. Liu *et al.* [10] found that the combination of V_2O_5 and TiO_2 (V_2O_5) not only facilitate the soot oxidation directly, but also oxidize NO to NO_2 in automobile exhaust like noble metal catalysts. Due to its strong oxidizing ability, the soot oxidation can be accelerated by NO_2. Here, the NO_2 is used as an intermediate to facilitate an indirect contact between the V_2O_5 and soot. At the same time, Neri *et al.* [11] believe that vanadium oxide catalyst may have a special reaction mechanism, namely, the catalyst separates partial oxygen atoms to form gaseous oxygen to enhance the oxidation reaction, and vanadium oxides can easily change the oxidation state, which can realize the catalytic cycle.

The nano-scale V_2O_5/TiO_2 catalysts with different loading rates were synthesized by impregnating the TiO_2 surface with V_2O_5 for DPF regeneration, which minimizes operational risks and energy consumption in engine applications [12]. This work aims at a comparative study on the phase structure and activity of different amount (5%, 10%, 20% and 40%) of V_2O_5 carried on the TiO_2 particles. The phase structure and surface species of V_2O_5/TiO_2 catalysts with different loading rates were characterized through scanning electron microscope (SEM), X-ray diffractomer (XRD) and fourier transform infrared spectroscopy (FT-IR). The performance of soot oxidation over vanadium-based catalysts is evaluated through thermogravimetric analysis (TGA). And then based on Flynn-Wall-Ozawa (FWO) method, the quantitative characterization of pyrolysis kinetics is carried out to explore the mechanism of soot oxidation process over vanadium-based catalysts, which will provide a theoretical basis for its real application in DPF.

2. Experimental

2.1. Preparation of catalysts and soot

The complicated catalysts of TiO_2 loaded by V_2O_5 with various fractions of 5 wt%, 10 wt%, 20 wt% and 40 wt% were prepared respectively by an impregnation method. These catalysts were named as V5, V10, V20 and V40. Nano-scale TiO_2-anatase produced by Shanghai Aladdin Reagent Co. Ltd. with a surface area of 71 m^2/g (BET method) was utilized as the support, due to its excellent sulfur resistance and electronic effects as compared with other supporters like Al_2O_3, ZrO_2, SiO_2 and so on. The catalysts, V_2O_5, were prepared by a standard wet impregnation method from NH_4VO_3 (Aladdin, Shanghai) dissolved in the aqueous oxalic acid (Aladdin, Shanghai) solution with a molar ratio of 1:2 to gain the aqueous solution. This aqueous solution was slowly heated by a magnetic stirrer until the color of solution gradually turned into dark blue, then the catalyst precursor was obtained. To this aqueous solution, the fine powder TiO_2 support was added and the blend ratio was 1 g/mL according to the water absorption of TiO_2, then we obtained the mixture. The mixture was oscillated for 30 minutes by an ultrasonic oscillator after uniformly impregnating and stirring treatment, then the mixture was stored at ambient temperature for 24 hours. Finally, it was dried for 12 hours at the temperature of 110 ^{o}C in an oven, and then it was calcinated for 5 hours at the temperature of 500 ^{o}C in a box-type resistance furnace.

Carbon black is often used as a substitute of diesel soot in evaluating the activity of catalysts on soot oxidation, since it has similar structure to diesel soot and owns ideal experimental repeatability. Therefore, Printex-U carbon black produced by Degussa was adopted to replace diesel soot in this study.

2.2. Characterization techniques

The microstructure of the catalysts was observed by using a JSM-7001F field emission SEM. Oxford Instruments (OIMS), UK. The crystalline phases of the catalysts were analyzed using an X-ray diffraction (BRUKER D8 ADVANCE with Cu-Kα radiation-40 kV, 40 mA) with 4 ℃/min scanning rate. NEXUS-470 FT-IR produced by Nicolet in America was used to analyze chemical composition of catalysts through 32 times scanning .The scanning range was 4000-400 cm^{-1} with a resolution of 4 cm^{-1}.

2.3. Thermegravimetric analysis

TGA/DSC1 thermogravimetric analyzer made by METTLER in Swiss was utilized to evaluate the performance of soot oxidation over nano-scale vanadium-based catalysts. Before the test, the mixture of catalyst and soot with a mass ratio of 5:1 was stirred adequately in the beaker to reach loose contact state. Soot oxidation in the presence of catalysts can be classified into three-phase reaction [13], which mainly occurs in the three-phase contact surface of soot particles, catalyst active sites and gaseous oxygen. The contact between catalysts and soot plays an important role in soot oxidation. A better contact can effectively increase the probability of contact between soot and the active sites of catalysts, and thus improve the catalytic efficiency [14]. Although tight contact can improve the performance of catalyst, the results may be unsatisfactory because this does not allow for a good representation of the real after treatment system [2]. Therefore, the loose contact of soot and catalysts was prepared and tested. Thermogravimetric test parameters were set as follows: the weight of the sample was about 4 mg, and the heating rate was set at 10 ^{o}C/min and temperature rising range was 40~800 ^{o}C, and the reaction gas was air with a flow rate of 50 mL/min.

3. Mathematical Modeling

Kinetic studies were performed in a thermogravimetric analyzer based on the non-isothermal Flynn-Wall-Ozawa (FWO) method. The thermal gravimetric experiments of soot in the presence of the catalyst V_2O_5 (V0, V5, V10, V20, V40) were performed at different heating rates (10, 15, 20, 25, 30 ^{o}C/min).

The homogeneous reaction dynamics equation [15] under isothermal conditions was basically completed by the end of the 19th century:

$$\frac{d\alpha}{dt} = k\, f(\alpha) \tag{1}$$

where: α is fraction of decomposition, $f(\alpha)$ is reaction mechanism function, and k is rate constant.

The rate constant k and temperature in dynamic equation have a great relationship. Ordinarily, the most used formula is the well-known Arrhenius formula as:

$$k = A\exp(-\frac{E}{RT}) \tag{2}$$

where: A is pre-exponential factor, R is the gas constant, (8.314 J/mol. K), and T is characteristic temperature (K), so the activation energy (E) (kJ /mol) could be determined.

From Equations (1) and (2), the commonly used dynamic equation under heterogeneous and non-isothermal conditions is:

$$\frac{d\alpha}{dT} = (\frac{A}{\beta})\exp(-\frac{E}{RT})\, f(\alpha) \tag{3}$$

In Equation (3), β indicates the heating rate (K/min). By integrating the both sides of Equation (3) on range of 0 to α and T_0 to T, the dynamic mechanism function in integral form can be given:

$$\int_0^\alpha \frac{d\alpha}{f(\alpha)} = G(\alpha) = \frac{A}{\beta}\int_{T_0}^{T} \exp(-\frac{E}{RT})dT \tag{4}$$

In Equation (4), $G(\alpha)$ stands for dynamic mechanism function in integral form. Considering the lower initial temperature T_0, the reaction rate can be neglected. Therefore, the integral range of 0 to T can instead of the range of T_0 to T Then, the Equation (4) can be rewritten to:

$$\int_0^\alpha \frac{d\alpha}{f(\alpha)} = G(\alpha) = \frac{A}{\beta}\int_0^{T} \exp(-\frac{E}{RT})dT \tag{5}$$

For $u=E/RT$, the above equation can be rearranged as in Equation (6):

$$G(\alpha) = \frac{A}{\beta}\int_0^{T} \exp(-\frac{E}{RT})dT = \frac{AE}{\beta R}\int_\infty^{u} \frac{-e^{-u}}{u^2}du = \frac{AE}{\beta R}\cdot P(u) \tag{6}$$

From the approximate equation of the thermogram calculated by Doyle [16], the approximate equation about $P(u)$ can be given as:

$$\ln P(u) \approx -5.3308 - 1.0516u \tag{7}$$

Then, combining Equations (6) and (7), the formula for FWO method is following [17, 18].

$$\ln\beta = \ln\frac{AE}{RG(\alpha)} - 5.3308 - 1.0516\frac{E}{RT} \tag{8}$$

Based on the calculation parameters and the Equation (8), the activation energy of soot oxidation can be achieved by the linear relationship between $\ln\beta$ and $1/T$.

$$y = \ln\beta \tag{9}$$

$$x = 1/T \tag{10}$$

$$a = -1.0516E/R \tag{11}$$

$$b = \ln\frac{AE}{RG(\alpha)} - 5.3308 \tag{12}$$

Then $\ln\beta$ and $1/T$ can be put into a linear equation of $y = ax + b$. The slope a can be worked out by drawing linear straight with a series of data points, subsequently the activation energy can be calculated by following formula:

$$E = -aR/1.0516 \tag{13}$$

4. Characterization of Catalysts

4.1. SEM characterization

The SEM micrographs of V_2O_5 catalysts with different loading rates are shown in Figure 1, in which the nano-scale carriers of TiO_2 is spherical with an average size of 25~30 nm. As expected, SEM images (Figure 1) show that the size of catalyst particles are remarkably increased with increase in the V_2O_5 content from 5 to 20 wt%. The particle size of V5, V10 and V20 are very tiny, which is less than 80 nm. However, the V40 catalyst presents more irregular columnar structures, which have sharp edges, bright surface and dense columnar structure, with the size ranging from dozens of nanometers to hundreds nanometers. It has been discovered that many supported catalysts have this widespread phenomenon that the active species can disperse on the surface of carrier to form a monolayer. However there is a monolayer dis-

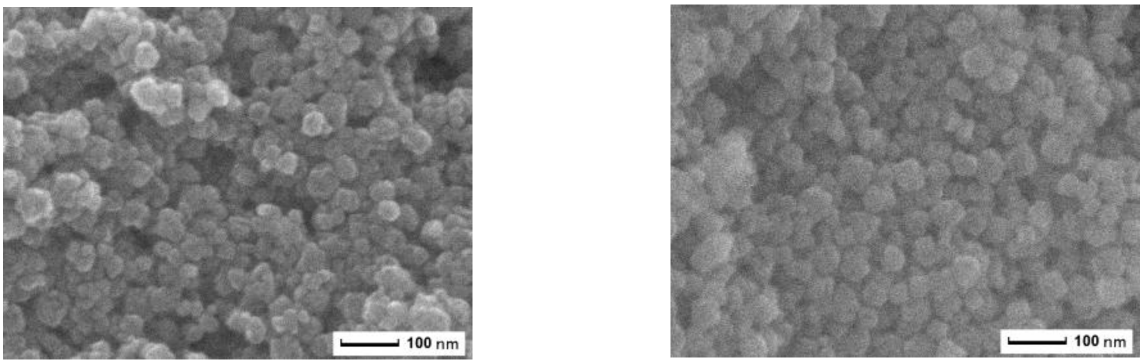

(a) TiO_2 (b) V5

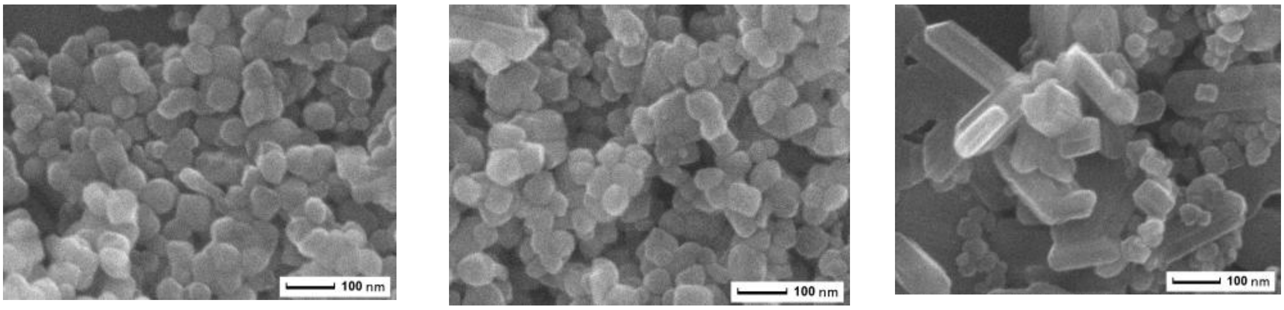

(c) V10 (d) V20 (e) V40

Figure 1. SEM images of V_2O_5 catalysts

persion capacity, i.e. monolayer dispersion threshold. When the loading of catalysts exceed the monolayer dispersion threshold, the crystalline of active species will form and cover the monolayer phase [19].

4.2. XRD characterization

Figure 2 is XRD patterns of complicated catalysts with V_2O_5 content of 0, 5, 10, 20, 40 wt%, respectively. As shown in Figure 2(a)-(e), the peaks detected at 2θ of 25.55°, 37.15°, 48.35°, 54.15° and 55.35° were believed to be due to the support, TiO_2. This perk pattern was in good accordance with XRD spectra of TiO_2-anatase crystal. This implied that the active components V_2O_5 did not destroy the crystal structure of the TiO_2. The absence of characteristic peak for V_2O_5 crystal (2θ = 20.26°) at V5 and V10 was due to the admirable dispersion of V_2O_5 in TiO_2 when the vanadium loading rate was low. Basically, they are in the monolayer distribution state and the vanadium oxides are mainly monomers and polymeric species [20]. Only when the V_2O_5 content was 20 wt% can the typical X-ray diffraction patterns of the V_2O_5 crystal be exactly detected. To further increase the catalyst loading, much more intense peak was detected, which indicated that V_2O_5 crystals grew up. In other words, the V_2O_5 is amorphous at a low loading content, while its crystallinity is increased at a higher loading content. The change of XRD phase structure with the V_2O_5 content in catalysts can be reasonably matched to the variety in SEM images.

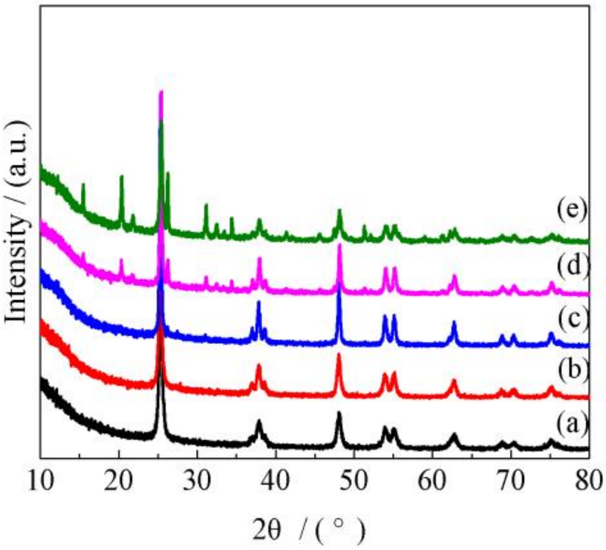

Figure 2. XRD spectra of V_2O_5 catalysts. (a) TiO_2, (b) V5, (c) V10, (d) V2, (e) V40

4.3. FT-IR characterization

FT-IR spectroscopy can reveal some information about structures of catalysts [9]. Figure 3 shows the FT-IR spectra of V_2O_5 catalysts with different loading rates. Two infrared transmission bands at 3400 cm^{-1} and 1630 cm^{-1}, which are attributed to the stretching modes of O–H in bound water and absorbed water and bending mode of water molecules, were observed in the spectra of catalysts. There was a very wide and intense band at 600 cm^{-1}, which was the vibration of Ti–O band in amorphous TiO_2, so the structure of carrier was not destroyed by the active species and the bands originating from the carrier did not interfere with the bands corresponding to the catalytic surface material [9]. It has been reported that at low vanadium loading monovanadates species were present on the surface of carrier and they were monolayer-dispersed systems [9, 19]. So the band at 1020 cm^{-1}, which is attributable to the V=O stretch vibration of V_2O_5 crystallites, was only detected at high vanadium loading rates (V20, V40). Bands in the range 1042-995 cm^{-1} are due to overtones and summation bands of the stretching modes of V=O in crystalline V_2O_5 [21]. Sharp and strong band at 1400 cm^{-1} appears in many literatures, but there is no consensus for which it belongs to [9, 22].

5. Activity Evaluation of V_2O_5 Catalyst

5.1. Catalytic performance under TG

The TG and DTG data of soot combustion in the presence of V_2O_5 catalysts with different

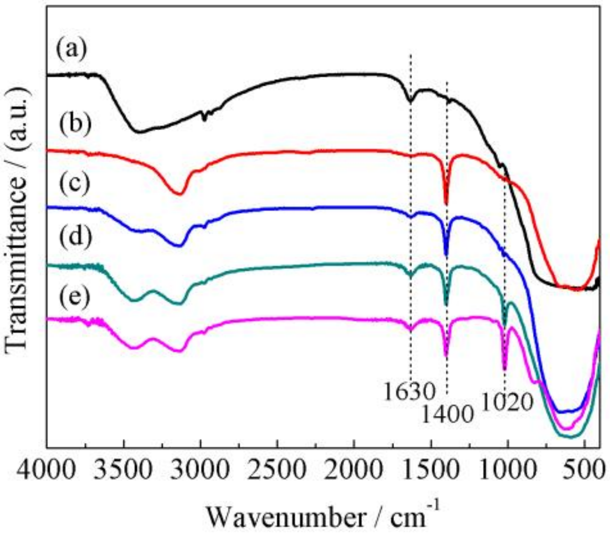

Figure 3. FT-IR spectra of V_2O_5 catalysts (a) TiO_2, (b) V5, (c) V10, (d) V20, (e) V40)

loading rates are shown in Figure 4. There was very little weight loss around 250 °C, which was due to water elimination [1]. Above 700 °C nearly no weight loss can be observed. So the soot was oxidized mainly at temperatures between 400 and 700 °C. The detailed characteristic parameters of soot weight less are listed in Table 1. In order to compare the activity of catalysts with various loading rates, the process of soot weight loss was evaluated by three characteristic temperatures: the light-off temperature (T_i), which corresponds to the initial 5 wt% of sample weight lost, the peak temperature (T_p) , which points to the maximum weight loss rate, and the burn-out temperature (T_b), which represents the end of soot oxidation.

According to the experimental data, although in loose contact, vanadium catalysts showed desirable catalytic activities by much reducing the light-off temperature (T_i) and peak temperature (T_p), compared with non-catalytic soot oxidation. This distinct performance of V_2O_5 catalysts may be resulted from the low melting point of V_2O_5. The active V_2O_5 species can form a liquid eutectic phase on the carrier surface and thus own favorable migration ability, which facilitates to improve the contact of catalysts with soot and then enhances the catalytic activity [1, 8, 9]. What's more, some researchers [1, 9] have discovered that the formation of surface oxygen complexes (SOC) at the interface of soot and V_2O_5 can greatly promote the oxidation of soot. Therefore, as shown in Figure 4, the TG and DTG profiles of soot with catalysts gradually shifted to lower temperatures and the characteristic temperatures were decreased with increasing V_2O_5 content from 0 to 20 wt%. To be noticed that the V40 profile traveled between the V20 and V10, which indicated the soot oxidation over V40 ran faster than V10 but slower than V20. This clearly reveals that the activity of catalysts is sensitively bound up with the loading amount of active species. The best activity was presented by the catalyst V20, which lowered the characteristic temperature T_i, T_p, and T_b by 69.1 ℃, 46 ℃ and 23 ℃, respectively. Therefore, the activity of catalysts can be ranked as follows: V5 < V10 < V40 < V20. According to the characterization results of SEM, FT-IR and XRD, the monolayer dispersion of catalysts in V20 appeared saturated. So, a threshold effect in vanadium-based catalysts can be affirmatively verified. Some researchers [9, 23] have studied the effect of V_2O_5 phase structure on its catalytic activity, and observed that polymeric and monovanadates species were active redox sites, which were more active than crystalline bulk vanadium oxide in catalytic reactions.

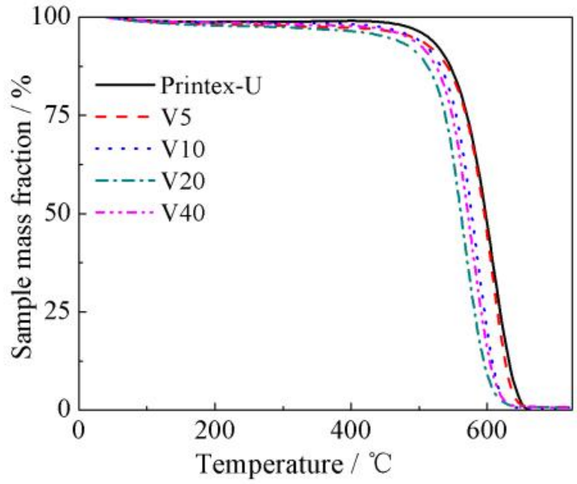

(a) TG Curve

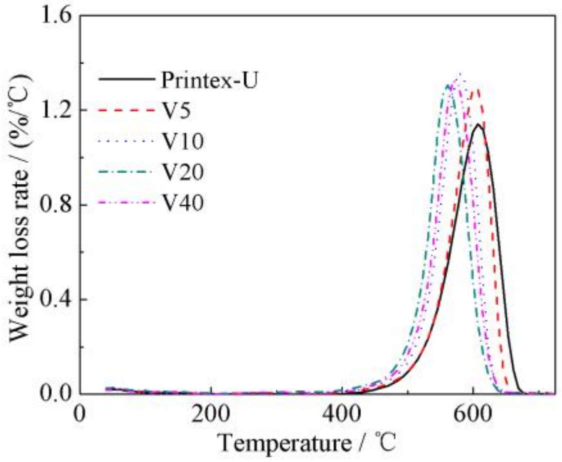

(b) DTG Curve

Figure 4. TG and DTG data of soot oxidation over V_2O_5 catalysts

Table1. Characteristics parameters of soot oxidation over V_2O_5 catalysts

Sample	Ignition temperature (T_i) /°C	Peak temperature (T_p) /°C	Burnout temperature (T_b) /°C	Weight loss peak /(%.°C^{-1})
soot	507.7	607.3	661.0	1.14
V5	492.3	599.7	653.3	1.29
V10	484.7	576.7	645.7	1.36
V20	438.6	561.3	638.0	1.31
V40	469.3	569.0	640.7	1.32

5.2. Pyrolysis kinetics

The thermal kinetic analysis aims to provide a quantitative expression to a reaction process (or phase change), to determine the most probable mechanism function that it follows, and to figure out the kinetic parameters such as the activation energy (*E*) and pre-exponential factor (*A*). The FWO method can present the activation energy (*E*) directly without involving dynamics model function. It can avoid the errors caused by different assumptions of the reaction mechanism function. Thus, it also can be called a model-free method. In recent years, this method has drawn a lot of attention.

DTG profiles of soot oxidation in presence of neat soot and the typical catalyst V20 are shown in Figure 5. The T_p at different heating rates obtained from experimental data were listed in Table 2. Based on the Equations (1)-(9), the plot of ln β versus $1/T_p$ for a certain sample, recorded at different heating rates, should be a straight line in theory, that is the square of the Pearson correlation coefficients (R^2) is equal to 1. And the activation energy values were able to obtain from the slope of the lines to evaluate the activity of different catalysts. The plots of ln β versus $1/T_p$ for different samples, obtained from TG and DTG data, were shown in Figure 6. Then the square of the Pearson correlation coefficients (R^2) and the activation energy values were calculated and given in Table 2. The plots for different samples are almost straight lines with $R^2 \geq 0.968$, which agrees with the requirement of FWO method [24, 25]

As shown in Table 2, the activation energy of soot combustion without catalyst is 175.5 kJ/mol, which is reasonable in statics [25]. The activation energy is supposed as the minimum energy needed to start a chemical reaction. In view of this terms, it is feasible to evaluate the activity of catalysts. According to the characterization results of SEM, XRD, and FT-IR, it is obviously found that polymeric vanadyl V–O–V species are active sites for soot oxidation reaction at a low vanadium loading. As a usual the concentration of polymeric vanadyl V–O–V species increases with the vanadium loading rate. So, the activation energy decreased with the increase in vanadium loading rate from 0 to 20 wt%. In general, high content of active species lead to the lower activation energy for soot oxidation over V5-V20. However, the activation energy was not always decreased with the increase in the active composition loading rate, especially for the catalyst V40. It is demonstrated that the active composition of the polymeric vanadyl V–O–V species was decreased and led to a reduction in the catalytic activity. This also can be indicated by the SEM, XRD and FT-IR re-

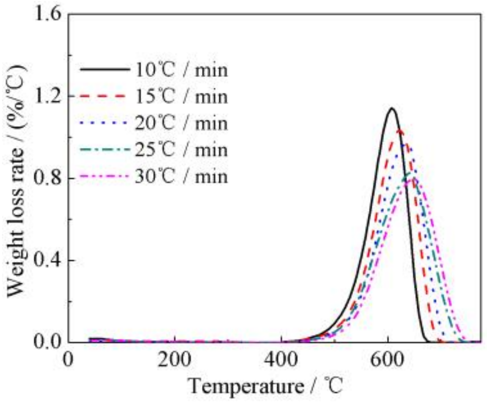

(a) soot

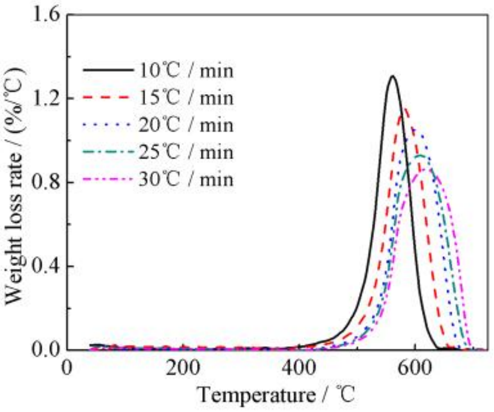

(b) V20

Figure 5. DTG data of soot oxidation at different heating rates

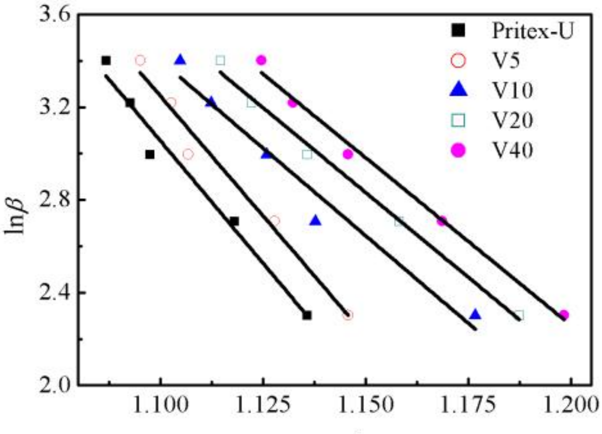

Figure 6. Fitting curves using FWO method

Table 2. Kinetic parameters of soot oxidation over V_2O_5 catalysts

Sample	T_p /K					Fitted lines	R^2	Activation energy (E) /(kJ·mol^{-1})
	10 °C /min	15 °C /min	20 °C /min	25 °C /min	30 °C /min			
soot	880.5	894.4	911.1	915.2	920.1	$y_1 = -21.11\,x_1 + 26.28$	0.9757	175.5
V5	872.8	886.7	903.5	906.9	913.4	$y_2 = -20.76\,x_2 + 26.00$	0.9774	171.9
V10	849.6	878.9	888.2	899.0	905.3	$y_3 = -15.10\,x_3 + 20.01$	0.9680	125.5
V20	834.4	855.6	872.8	883.2	889.2	$y_4 = -14.44\,x_4 + 19.59$	0.9922	120.0
V40	842.2	863.3	880.4	891.1	897.6	$y_5 = -14.63\,x_5 + 19.66$	0.9928	121.6

sults, which reveal the formation of crystalline structure as the loading rate of V_2O_5 exceeds V20. The V_2O_5 in crystalline structure is less active than polymeric vanadyl species. Among all the experimented samples, the activation energy for soot oxidation over V20 (120.0 kJ/mol) is the lowest, i.e. it owns the highest activity. This confirms that there is an obvious threshold effect in V_2O_5 catalysts.

6. Conclusions

The loading rates have great effects on the phase structure and catalytic activity of V_2O_5 catalysts. At low V_2O_5 loading rates, they are in the monolayer distribution and the vanadium oxides are monomers and polymeric, and the catalytic activity of V_2O_5 increases with the increase in V_2O_5 loading rate. When V_2O_5 loading rates outnumber 20 wt%, crystalline bulk V_2O_5 forms on the surface of the carrier, which causes the catalytic activity decreased. Based on the characteristic temperatures of soot oxidation for each sample, the order of the catalyst activity can be obtained as follows: V5 < V10 < V40 < V20. There is an obvious threshold effect in the V_2O_5 catalysts.

Based on the FWO method, the soot oxidation over V_2O_5/TiO_2 catalysts was quantitatively characterized. With increasing V_2O_5 loading, the activation energy needed for soot oxidation is decreased in an order $E_{soot} > E_{V5} > E_{V10} > E_{V40} > E_{V20}$, which fits well with the results of catalysts characterization. For the catalysts in this study, the minimum activation energy of soot oxidation is 120.04 kJ/mol when the vanadium loading rates is 20 wt%.

Acknowledgment

The authors wish to express their appreciation for the funds from the National Natural Science Foundation of China (No. 51376095 and No. 51506101), which supported this study.

References

[1] Leocadio, I.C.L., Braun., S., Schmal, M. (2004). Diesel soot combustion on Mo/Al_2O_3 and V/Al_2O_3 catalysts: investigation of the active catalytic species. *Journal of Catalysis*, 223(1): 114-121.

[2] Toniolo, F., Elisa, B., Schwaab, M., Leocadio, I., Aderne, R., Schmal, M., Pinto, J. (2008). Kinetics of the catalytic combustion of diesel soot with MoO_3/Al_2O_3 catalyst from thermogravimetric analyses. *Applied Catalysis A: General*, 342(1-2): 87-92.

[3] Prasad, R., Bella, V.R. (2010). A review on diesel soot emission, its effect and control. *Bulletin of Chemical Reaction Engineering & Catalysis*, 5(2): 69-86 (DOI: 10.9767/bcrec.5.2.794.69-86)

[4] Rao, T.V.M., Vico-Ruiz, E., Bañares, M.A., Deo G. (2008). Obtaining the best composition of supported V_2O_5–MoO_3/TiO_2 catalyst for propane ODH reaction. *Journal of Catalysis,* 258(2):324-333

[5] Albonetti, S., Blasioli, S., Bruno, A., Epoup, Mengoua, J., Trifirò, F. (2006). Effect of silica on the catalytic destruction of chlorinated organics over V_2O_5/TiO_2 catalysts. *Applied Catalysis B: Environmental*, 64(1-2): 1-8.

[6] Lin, Y.C., Chang, C.H., Chen, C.C., Jehngc, J.M., Shyu, S.G. (2006). Supported vanadium oxide catalysts in selective oxidation of ethanol: Comparison of TiO_2/SiO_2 and ZrO_2/SiO_2 as supports. *Catalysis Communications*, 64(1-2): 1-8.

[7] Woojoon, C., Sungmin, C., Eunseuk, P., Yunb, S.T., Jurng, J. (2013). Effect of V_2O_5 loading of V_2O_5/TiO_2 catalysts prepared via CVC and impregnation methods on NO_x removal. *Applied Catalysis B: Environmental*, 140-141: 708-715.

[8] Uchisawa, J., Obuchi, A., Ohi, A., Nanba, T., Nakayama, N. (2008). Activity of catalysts supported on heat-resistant ceramic cloth for diesel soot oxidation. *Powder Technology*, 180(1-2): 39-44.

[9] Liu, J., Zhao, Z., Xu, C.M., Duana, A.J., Zhu, L. Wang, X.Z. (2005). Diesel soot oxidation over supported vanadium oxide and K-promoted vanadium oxide catalysts. *Applied Catalysis B: Environmental*, 61(1-2): 36-46.

[10] Liu, J., Zhao, Z., Peng, L., Xu, C.M., Duan, A.J., Jiang, G.Y., Lin, W.Y., Wachs, I.E. (2008). Study on the reaction mechanism for soot oxidation over TiO_2 or ZrO_2-supported vanadium oxide catalysts by means of In-situ UV-Raman. *Catalysis letters*, 120(1-2): 148-153.

[11] Neri, G., Rizzo, G., Galvagno, S., Musolinob, M.G., Donatob, A., Pietropaolo, R. (2002). Thermal analysis characterization of promoted vanadium oxide-based catalysts. *Thermochimica Acta*, 381(2): 165-172.

[12] Lopez-Fónseca, R., Elizundia, U., Landa, I., Gutiérrez-Ortiz, M.A., González-Velasco, J.R. (2005). Kinetic analysis of non-catalytic and Mn-catalysed combustion of diesel soot surrogates. *Applied Catalysis B: Environmental*, 61(1-2): 150-158.

[13] Zhao, Z., Zhang, G.Z., Liu, J., Liang, P., Xu, J. (2008). Latest research progresses in catalysts for the purification of exhaust gases from diesel engines. *Chinese Journal of Catalysis*, 29(3): 303-312.

[14] Hensgen, L., Stöwe, K. (2011). Soot-catalyst contact studies in combustion processes using nano-scaled ceria as test material. *Catalysis Today*, 159(1): 100-107.

[15] Vyazovkin, S. (2000). Kinetic concepts of thermally stimulated reactions in solids: A view from a historical perspective. *International Reviews in Physical Chemistry*, 19(1): 45-60.

[16] Doyle, C.D. (1961). Kinetic Analysis of Thermogravimetric Data. *J. Appl. Polym. Sci*, 5(15): 285-92.

[17] Ozawa, T. (1965). A new method of analyzing thermogravimetric data. *Bull. Chem. Soc. Jpn.*, 1965, 38(11): 1881-1886.

[18] Flynn, J.H., Wall, L.A. (1966). A quick, direct method for the determination of activation energy from thermogravimetric data. *Journal of Polymer Science Part B: Polymer Letters*, 4(5): 323-328.

[19] Wang, X., Zhao, B., Jiang, D.E., Xie, Y.C. (1999). Monolayer dispersion of MoO_3, NiO and their precursors on γ-Al_2O_3. *Applied Catalysis A: General*, 188(1): 201–209.

[20] Liu, X.J., Gu, X.D., Shen, J.Y. (2003). Structure, surface acidity/ basicity and redox properties of V_2O_5/TiO_2 catalysts. *Chinese Journal of Catalysis*, 24(9): 674-680.

[21] Singh, S., Jonnalagadda, S.B. (2008). Selective oxidation of n-Pentane over V_2O_5 supported on hydroxyapatite. *Catalysis Letters*, 126(1-2): 200-206.

[22] Li, C., Zhang, H., Wang, K.L., Qin, X. (1994). FT-IR emission spectroscopic studies of surface structure of V_2O_5/TiO_2 catalyst. *Acta Physico-Chimica Sinica*, 10(1): 33-37.

[23] Alvarez-Puebla, R.A., Garrido, J.J., Aroca, R.F. (2004). Surface-enhanced vibrational microspectroscopy of fulvic acid micelles. *Analytical Chemistry*, 76(23): 7118-7125.

[24] Yezerets, A., Currier, N.W., Kim, D.H., Eadlera, H.A., Eplinga, W.S., Peden, C.H.F. (2005). Differential kinetic analysis of diesel particulate matter (soot) oxidation by oxygen using a step–response technique. *Applied Catalysis B: Environmental*, 61(1-2): 120-129.

[25] Sharma, H.N., Pahalagedara, L., Joshi, A., Suib, S.L., Mhadeshwar, A.B. (2012). Experimental study of carbon black and diesel engine soot oxidation kinetics using thermogravimetric analysis. *Energy Fuels* 26(9): 5613-5625.